JOURNAL OF SPACECRAFT AND ROCKETS
Vol. 46, No. 6, November–December 2009

Sensitivity of Orbit Predictions to Density Variability

Rodney L. Anderson,* George H. Born,† and Jeffrey M. Forbes‡
University of Colorado, Boulder, Colorado 80309

DOI: 10.2514/1.42138

This paper summarizes the first stage in a research effort designed to obtain a quantitative knowledge and deeper understanding of how prediction error depends on density variability. Initial numerical simulations are performed to obtain a detailed understanding of the theoretical effects of density variations on satellite orbit predictions. The level of knowledge of density variations needed for various orbit prediction requirements is quantified, and results are compiled focusing on the effects of various horizontal wavelengths in the atmosphere. The information obtained in this analysis lays the foundation for the next step of connecting the simulation results to the prediction of actual satellite ephemerides.

Nomenclature

A	=	area, m^2
A_p	=	average daily planetary geomagnetic index
$\mathbf{a}$	=	acceleration, m/s^2
$\mathbf{a}_{\text{drag}}$	=	acceleration due to drag, m/s^2
a_p	=	3 h planetary geomagnetic index
C_d	=	drag coefficient
$\mathbf{F}$	=	force, N
f	=	fraction of the nominal density at a specified altitude
$\mathbf{I}$	=	impulse, kg m/s
m	=	mass, kg
$\mathbb{P}$	=	period of the spacecraft computed from the initial conditions without taking drag into account, h
t_f	=	final time, s
t_i	=	initial time, s
$\mathbf{V}$	=	velocity, m/s
V_a	=	velocity magnitude relative to the atmosphere, m/s
$\mathbf{V}_a$	=	velocity relative to the atmosphere, m/s
$\dot{x}$	=	x component of the velocity in the inertial frame, m/s
$\dot{y}$	=	y component of the velocity in the inertial frame, m/s
$\dot{z}$	=	z component of the velocity in the inertial frame, m/s
$\Delta\mathbf{V}$	=	change in velocity, m/s
$\dot{\theta}$	=	rate of the Earth's rotation, rad/s
ρ	=	atmospheric density, kg/m^3
ρ_{nom}	=	nominal density at a specified altitude, kg/m^3

I. Introduction

AS DENSITY models have improved in terms of temporal and spatial resolution, they have become an integral part of the orbit prediction process, and they have resulted in greatly improved accuracies for these predictions. With current research initiatives focused on improving the accuracy of density models even further, one natural question that arises is to what level do improved density models result in improved orbit predictions? More specifically, does increased knowledge of all minor density variations result in improvements, or is a rough knowledge of these variations sufficient? This leads to additional questions related to what sorts of variations are more important. For example, is emulating spatial accuracy or temporal accuracy in the model predictions worth more effort? For orbit determination, the altitudes, and correspondingly the orbit types, for which these effects are noticeable becomes important. These are some of the primary items of interest under the umbrella of this study. One goal of this program includes obtaining a quantitative knowledge and deeper understanding of how prediction error depends on density variability. One of the ultimate objectives is to connect simulation results to the prediction of actual satellite ephemerides. Before diving into these topics, it is worth reviewing the significant body of work related to the current state of density modeling and applications to orbit prediction.

Although it has typically been possible for most satellite missions to tailor their requirements to work with the current state of the art in atmospheric model predictions, there have been several cases where the predictions proved inadequate. After the magnetic storm on 13–14 March 1989, significant difficulties were encountered in tracking satellites. An important source of this problem was the inability of the models to accurately predict the atmospheric density changes as a result of the storm. Marcos [1] and Marcos et al. [2] provide a more detailed overview of the accuracy of current atmospheric drag models. In 1972, Forbes studied the effect of phase errors in the density model on the prediction of the location of the DB-7 satellite [3]. The plots showing the effect of the different density models on the orbit predictions are reproduced in Fig. 1. The plots reveal that a premature density increase predicted by the Jacchia model [4] actually resulted in as large of an error as simply predicting no variation at all. Although the quarter-day delays seen in the density model in Fig. 1 are no longer common, 1–4 h delays are still possible and potentially significant. The effects seen in this paper are typically much smaller than those seen in the plots, but they serve as an extreme example of the potential effects of modeling the atmosphere incorrectly.

One question that naturally arises relates to which horizontal density structures are of greatest importance or which ones have the greatest effect on orbit predictions. Forbes [5] and Rhoden et al. [6] analyzed data from the Satellite Electrostatic Triaxial Accelerometer experiment to investigate these structures. The satellite was at an altitude of between 170 and 220 km, and the data they analyzed were from the summers of 1982 and 1983. The wave scales they found to be of the most interest, or the most common in the data, ranged from about 150 to 2500 km. Others have found the existence of large scale ($\approx$1000 to $\approx$ 4000 km) and medium scale ($\approx$100 to $\approx$ 500 km) horizontal wavelengths to be of interest [7]. Using the Challenging Minisatellite Payload (CHAMP) data, Sutton et al. [8–10] and Sutton [11] noticed that for the particularly active year of 2003 scales on the order of approximately 1000 or 8000 km wavelengths were significant. Note that this significance was typically evaluated by examining the power spectral densities to determine which scales were more likely to be encountered.

Presented as Paper 6443 at the AIAA/AAS Astrodynamics Specialist Conference and Exhibit, Honolulu, HI, 18–21 August 2008; received 18 November 2008; accepted for publication 15 July 2009.

*Research Associate, Colorado Center for Astrodynamics Research, Aerospace Engineering Sciences. Member AIAA.

†Director, Colorado Center for Astrodynamics Research, Aerospace Engineering Sciences. Fellow AIAA.

‡Glenn Murphy Professor, Aerospace Engineering Sciences. Associate Fellow AIAA.

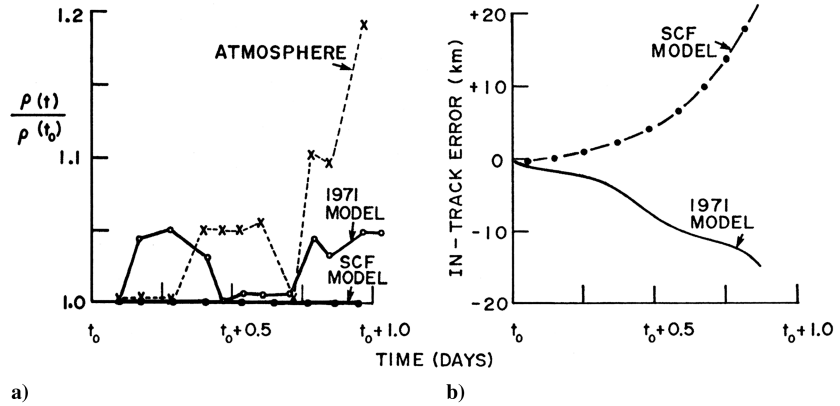

Fig. 1 Shown are the following: a) actual density variation from orbital analysis of the low-perigee (~170 km) satellite DB-7, the density variation from a purely static (U.S. Standard or Satellite Control Facility) model, and the 1971 (Jacchia or J71) model, and b) predicted in-track position errors (actual minus predicted) for the same time interval [3].

The U.S. Air Force and others have been improving density models for their orbit predictions for quite some time [12–19]. For this study, the primary motivation for density model improvements is tied to the U.S. Air Force prediction requirements. Errors for a 24 h prediction have been classified as significant for their purposes relative to the orbit altitude. The approximate errors of concern for several orbit altitudes are listed in Table 1. This study focuses on determining the density variations that would produce errors of concern for the U.S. Air Force as shown in the table, while also keeping in mind other applications for which the requirements may be more stringent.

The research presented here summarizes one of the first steps in the process of connecting simulation results to the prediction of actual satellite ephemerides, with a focus on numerical simulations using actual density data from the CHAMP spacecraft. These numerical simulations are performed to obtain a detailed understanding of the theoretical effects of density variations on satellite orbit predictions. They allow an isolation of the density variation effects that might be more difficult to do with actual satellite data. This knowledge can also aid in the validation of algorithms as they are added to more detailed models in the Global Positioning System (GPS)-Inferred Positioning System Orbit Analysis and Simulation software [20]. Initially, earlier research [3] showing the importance of capturing the temporal variations in density for increased solar activity in the case of a real satellite was analyzed to lay the background for this work. The first part of this study focuses on performing several simple simulations using standard exponential models with different types of density variations superimposed on the model. The orbit prediction accuracies obtained using the U.S. Naval Research Laboratory Mass Spectrometer and Incoherent Scatter Radar (NRLMSISE-00) model [21] compared with the CHAMP densities are then examined. Next, the "truth" results obtained using the CHAMP density data are compared with the orbit prediction results with a smoothed version of the density model. Overall, this study examines the importance of capturing the larger variations in the density with regard to horizontal scales and attempts to determine the knowledge of density variations needed for various orbit prediction requirements. The research presented here seeks to quantify the effect of smaller density variations and provide estimates of the sorts of errors expected, along with the model accuracies needed for different types of applications. These results directly inform the atmosphere modelers about the required resolutions as they model horizontal scales in the density variations and allow them to focus their efforts appropriately.

Table 1 24 h orbit prediction errors of significance to the U.S. Air Force for several altitudes

Altitude, km	Error, m
200	>250
400	>100
800	>50

II. Models

A. Two-Body Model with Drag

Acceleration due to drag (or force per unit mass) is

$$\mathbf{a}_{\text{drag}} = -\tfrac{1}{2}(C_d A/m)\rho V_a \mathbf{V}_a \tag{1}$$

where $m/(C_d A)$ is referred to as the ballistic coefficient. The velocity relative to the atmosphere may be computed as

$$\mathbf{V}_a = \begin{bmatrix} \dot{x} + \dot{\theta} y \\ \dot{y} - \dot{\theta} x \\ \dot{z} \end{bmatrix} \tag{2}$$

If the Earth's rotation is assumed to be zero, this becomes simply the inertial velocity vector

$$\mathbf{V}_a = \begin{bmatrix} \dot{x} \\ \dot{y} \\ \dot{z} \end{bmatrix} \tag{3}$$

B. Impulse and ΔV from Density Perturbations

The concept of the impulse or the change in the momentum of the spacecraft will be useful.

$$\mathbf{I} \equiv \int_{t_i}^{t_f} \mathbf{F}\,\mathrm{d}t \tag{4}$$

The equations in our case typically have the mass divided out, which reduces the relationship to

$$\Delta\mathbf{V} \equiv \int_{t_i}^{t_f} \mathbf{a}\,\mathrm{d}t \tag{5}$$

As an example, consider a sine wave density cycle integrated over one period. This may be written as

$$\Delta V = \int_0^{\mathbb{P}} -\frac{1}{2}\frac{C_d A}{m}\rho V_a^2\,\mathrm{d}t \tag{6}$$

Now, given a sine wave perturbation amplitude equal to some fraction (f) of the nominal density at the specified altitude, the equation for density is

$$\rho = f\rho_{\text{nom}} \sin(2\pi t/\mathbb{P}) \tag{7}$$

If k density cycles are desired per period, the density may be written as

$$\rho = f\rho_{\text{nom}} \sin(2\pi kt/\mathbb{P}) \tag{8}$$

Combining and integrating for an arbitrary time period gives

$$\Delta V = \int_{t_i}^{t_f} -\frac{1}{2}\frac{C_d A}{m} f\rho_{\text{nom}} \sin\left(\frac{2\pi kt}{\mathbb{P}}\right) V_a^2 \, \mathrm{d}t \tag{9}$$

$$\Delta V = -\tfrac{1}{2}(C_d A/m)V_a^2 f\rho_{\text{nom}}[\mathbb{P}/(2\pi k)] \times [-\cos(2\pi kt_f/\mathbb{P}) + \cos(2\pi kt_i/\mathbb{P})] \tag{10}$$

Naturally, integrating for the entire period should give zero for the result, so that one case of interest is to integrate for half the period.

Now it is interesting to ask the question related to what constant acceleration over this time period would result in the same $\Delta\mathbf{V}$. This may be computed from

$$\Delta\mathbf{V} = \mathbf{a}\Delta t \tag{11}$$

Remember that this formulation is only taking into account density effects above and beyond the nominal density. Reformulating Eq. (11) to investigate the effect of different function shapes is also relatively straightforward.

III. Challenging Minisatellite Payload

A. Spacecraft

The results presented here are all obtained using the CHAMP orbit and spacecraft parameters. The CHAMP spacecraft was launched into a low Earth orbit on 15 July 2000 [22,23]. Its initial altitude was 454 km, and it had an inclination of approximately 87 deg. Its total mass at launch was 522 kg, which dropped to approximately 505–507 kg in 2003.

As only approximate numbers are needed for the simulations in this paper, a mass of 522 kg is used along with an area-to-mass ratio of 0.00138 m^2/kg. For the simulations in this study, a drag coefficient of 2 is assumed, and this satellite is taken as a representative satellite for this analysis. Note that, if precise values are desired for the drag coefficient, Sutton recently showed that they may vary from about 2.3 to 3.7 [24]. Note also that ballistic coefficients for some satellites may typically be half as large as the value used here, and the orbit differences given next will show corresponding increases for such satellites. CHAMP possesses onboard an advanced, codeless, dual-frequency GPS receiver, called the Blackjack receiver, used for precision orbit determination. Significant effort has gone into processing the CHAMP accelerometer data and producing estimated densities and winds (see Sutton et al. for more information [8,9]). The data processed in these studies are the data used as the basis for the CHAMP analyses in this paper.

B. Data

Significant work has been done to analyze the CHAMP data by Sutton in his dissertation [11]. By analyzing the power spectral density over different orbits, he determined that two horizontal wavelengths were of particular importance or the most common. These wavelengths were at approximately 1000 and 8000 km. These wavelengths will be a focus for some of the studies performed in this paper. His dissertation focused on the CHAMP data from 2003, so that much of this analysis is performed for the same year. One interesting feature during this year was a series of geomagnetic storm peaks in the last days of October and a separate large storm event in November.

More recently, Sutton et al. analyzed the CHAMP data along with the models to determine the types of time delays that are introduced into the models [10]. The specific time delay that is of interest here is the time delay between the occurrence of a storm and the prediction of the storm in the models. Some of these time delays in the model come from the fact that the a_p indices are only available every 3 h. Their study showed that delays from 1 to 4 h exist near the equator, and delays from 1 to 2 h exist at the mid-to-upper latitudes. The 1 h delays are achieved by using interpolation of the a_p values.

This study focuses on an active year (2003) and a relatively quiet year (2007) to determine how the results vary based on solar activity. The year 2003 is especially convenient because Sutton [11] has already done an extensive analysis of the density data itself in his thesis, and statistics are readily available. Although most of the following analysis covers an entire year, it is useful to look at the densities and results for particular days. It would be preferable to focus on one geomagnetically quiet day and one geomagnetically active day. The data quality should also be acceptable for the days in question. The question of data quality may be answered by plotting the number of points requiring interpolation in the attitude of the spacecraft each day and the number of these data points processed each day. Note that each data point corresponds to a measurement that includes the attitude of the spacecraft and the measurements related to density. Generally, no more than 1000 points should require interpolation in the spacecraft attitude, and at least 8000 data points should be processed each day. See Sutton's dissertation for the reasoning behind this criteria [11]. These statistics are plotted in Fig. 2. The level of geomagnetic activity is evaluated by plotting A_p over 2003 in Fig. 3a. Using the information in these plots, two days were selected: 24 June 2003 (day of year = 175, $A_p = 23$) and

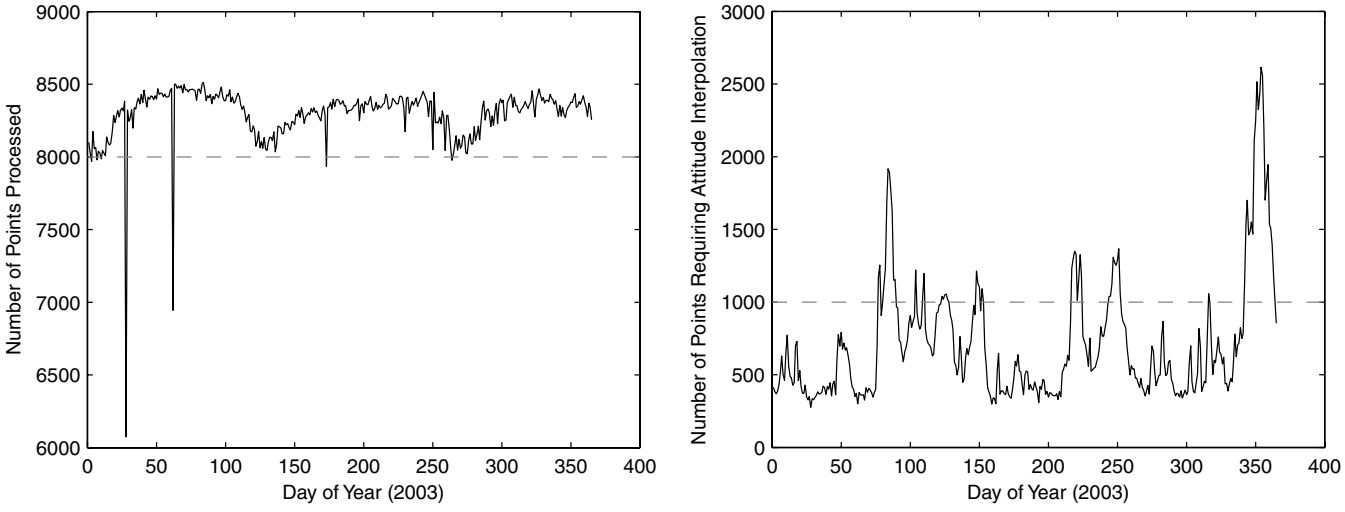

Fig. 2 Plots of statistics describing the quality of the data. No more than 1000 points should require interpolation in the attitude of the spacecraft each day, and at least 8000 points should be processed each day.

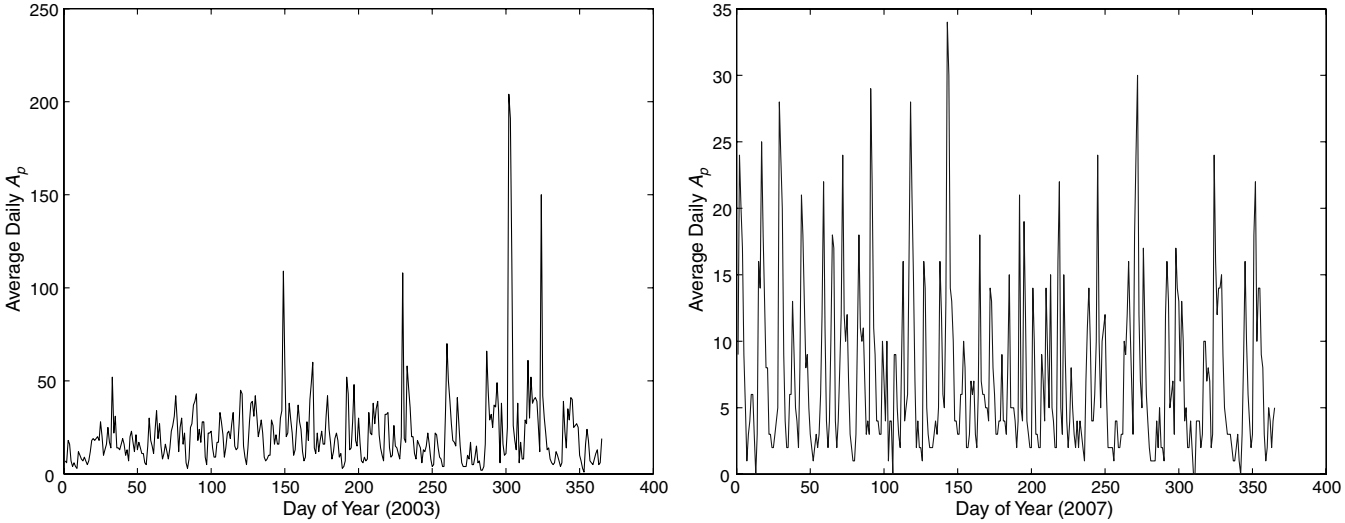

a) b)

Fig. 3 A_p values for each year.

20 November 2003 (day of year = 324, $A_p = 150$). The F10.7 values adjusted to 1 AU for days 175 and 324 were 118.3×10^{-22} and 171.0×10^{-22} W/m^2/Hz, respectively. This selection gives one case that has high geomagnetic activity and one that has more average geomagnetic activity. Examining a year that is geomagnetically quiet is also useful. The year 2007 was selected for this analysis, and the A_p values are plotted in Fig. 3b. As can be easily seen from a comparison with Fig. 3a, these values are generally much smaller and do not possess the peaks found during 2003.

IV. Modeling Density Perturbations with Different Functions

Our overall methodology consists of starting with the simplest cases and building up to the most complicated. This paper is the first step in that process of building up to orbit predictions with a full gravity model and density models. This method is followed here by first examining the effect of horizontal wavelengths using simple functions before moving on to comparing orbit predictions with model densities and actual CHAMP density measurements. This process then sets the stage for comparing actual CHAMP density measurements with smoothed versions of that data.

More specifically, one of the primary objectives of this study is to examine the importance of the wavelengths of density perturbations on the prediction of orbits and to determine which wavelengths have the most effect on this process. In addition to this, quantifying the effects of density perturbation scales allows an estimation of its importance relative to other effects such as phase offsets. This problem is attacked here first in a theoretical sense by examining the effect of using analytical functions to model density perturbations. The use of analytical functions such as sine waves, with which the wavelength may be modified, allows the effect of this one factor on the orbit prediction to be isolated. This should provide a theoretical basis for understanding the effects of density perturbation scales when actual data from satellites such as CHAMP are introduced into the analysis.

The effect of the density perturbation wavelengths on the orbit of a satellite was further isolated by using a simple model. In this model, a spacecraft was set in motion about the Earth modeled as a point mass. The 1976 Standard Atmosphere [25] was used to compute a density at the altitude corresponding to the initial conditions of the spacecraft. Initially, circular orbits were used, and the spacecraft was integrated forward for selected time periods. The case in which the spacecraft is integrated forward using a constant density is always referred to as the nominal case. For these first test cases, an inertially fixed atmosphere was used with no Earth rotation. This allowed one complete revolution of the spacecraft in its orbit to correspond to a complete circumscription of the desired density variations. Using this method, the spacecraft will be ensured to encounter an integer number of density perturbation cycles. This ensures that the average density encountered by the spacecraft using the nominal atmosphere and the spacecraft using the perturbed atmosphere should be the same. Note that, for the sine wave case, a density perturbation cycle would be one period of a sine wave.

One small assumption in this portion of the study should be noted here. The expectation is that the two spacecraft will follow slightly different paths due to the differences in the densities, and one will most likely have descended more than the other at the end of the simulation. For this portion of the study, the densities were simply made a function of the longitude, and the variation of density due to height was neglected. For the perturbations used in the majority of the cases selected here, the variations in height are expected to be slight over the tested time periods. The variations in height that might typically be observed in these cases were on the order of meters or tens of meters for some of the longer integrations.

Three different functions were examined primarily with the goal of determining whether changing the function shape has a large effect on the orbit prediction results. These functions included sine waves, step functions, and multiple impulsive ΔV. Schematics of the different functions compared with the constant density are shown in Fig. 4. For this initial comparison, using different density perturbation functions, all integrations were performed for one period.

A. Sine Wave

As explained earlier, for the sine wave case a sine wave density perturbation was superimposed upon the nominal constant density at the specified altitude. For this initial analysis, a 400 km circular orbit was used to roughly approximate the orbit of the CHAMP satellite. This results in a period of approximately 1.54 h. The sine wave perturbation was given an amplitude equal to 25% of the nominal density. The density used for 400 km was approximately 2.8×10^{-12} kg/m^3. The nominal case was the trajectory integrated for one period with this constant density. The perturbed case was integrated from the same initial state with the sine wave variation included in the atmosphere. The perturbed and nominal cases were compared for different density perturbation wavelengths. The resulting differences in the orbits for three sample cases with one, two, and three density perturbation cycles are shown in Fig. 5. The cross-track differences are zero for each of these cases because no drag is acting in the cross-track direction. As expected, the largest difference between the two orbits in each case is in the in-track direction. Comparing the final position differences reveals that the case with one density cycle appears to have a significantly larger

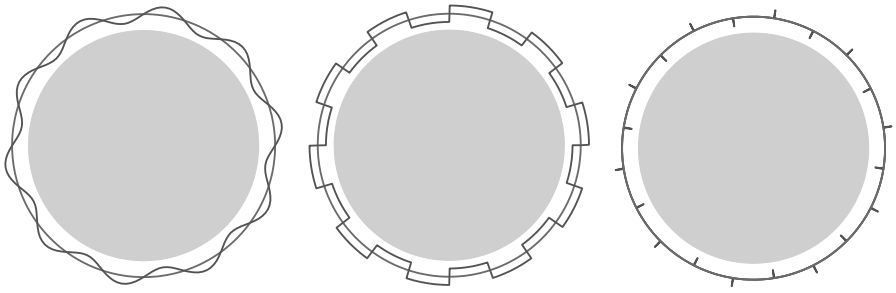

a) Sine wave b) Step c) Impulsive ΔV

Fig. 4 Schematics of sine wave and step density fluctuations computed so that an integer number of density cycles are encountered in one orbit. The impulsive ΔV case schematic indicates the locations where multiple ΔV are imparted to mimic the density fluctuations.

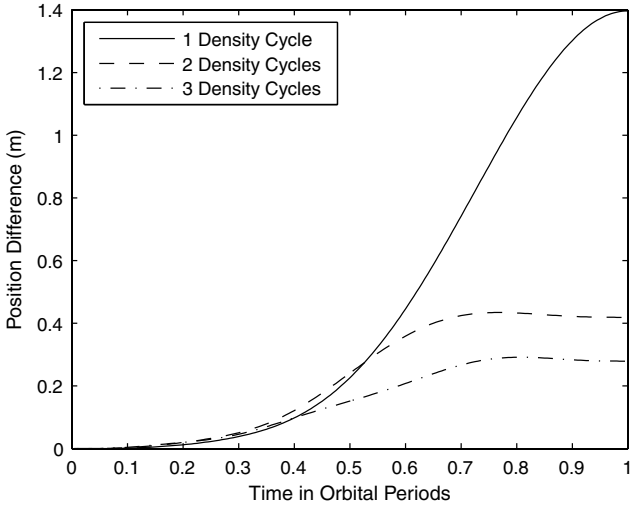

Fig. 5 Total position difference from the nominal orbit over time. The position difference was dominated by the in-track differences as expected. The integration period was for one complete orbital period with one, two, and three sine wave density cycles.

difference than the other cases. A comparison of the final orbit differences was performed for a much larger set of wavelengths, and the results are summarized in Fig. 6 and 7. Examining the trends in the data reveal that, with the exception of one case, the ratio of the final position difference to the density wavelength remains nearly constant with an average value of approximately 1.9682×10^{-8}. The one exception to this is the case with one density cycle for one orbit revolution. In this case the ratio is 3.279×10^{-8}. Thus, in general, given the wavelength, the final orbit difference can be approximately computed. The change in slope between the one and two density cycle cases appears to be due to some nonlinear effects that become apparent only as the density perturbation wavelengths grow larger. The slope of this curve also appears to be a function of the wavelength and the propagation time.

Examining the magnitude of the orbit differences shows that the maximum value occurs for the one density cycle case, and it results in a 1.4 m difference. This result indicates that if perturbations on this scale were not taken into account, the resulting predicted orbit would be 1.4 m off. This scale length, however, is rather larger than the lengths that have been previously discussed. As mentioned earlier, the scales that are of more interest are on the order of several thousand kilometers. Examining Fig. 7b reveals that wavelengths of this size could result in errors on the order of 0.1 m. This result, however, is just for one orbit, and so longer integration times (24–72 h) will need to be examined.

B. Step Function

The next function chosen for the comparison was the step function. This function was chosen because it is significantly different in shape from the sine function, and if the shape of the function is to have a large effect on the results it would likely show up for this case. The step function was chosen so that it was positive when the sine wave function was positive and negative when the sine wave was negative. Choosing a magnitude for the step function to obtain a proper comparison is worth some discussion. The simplest

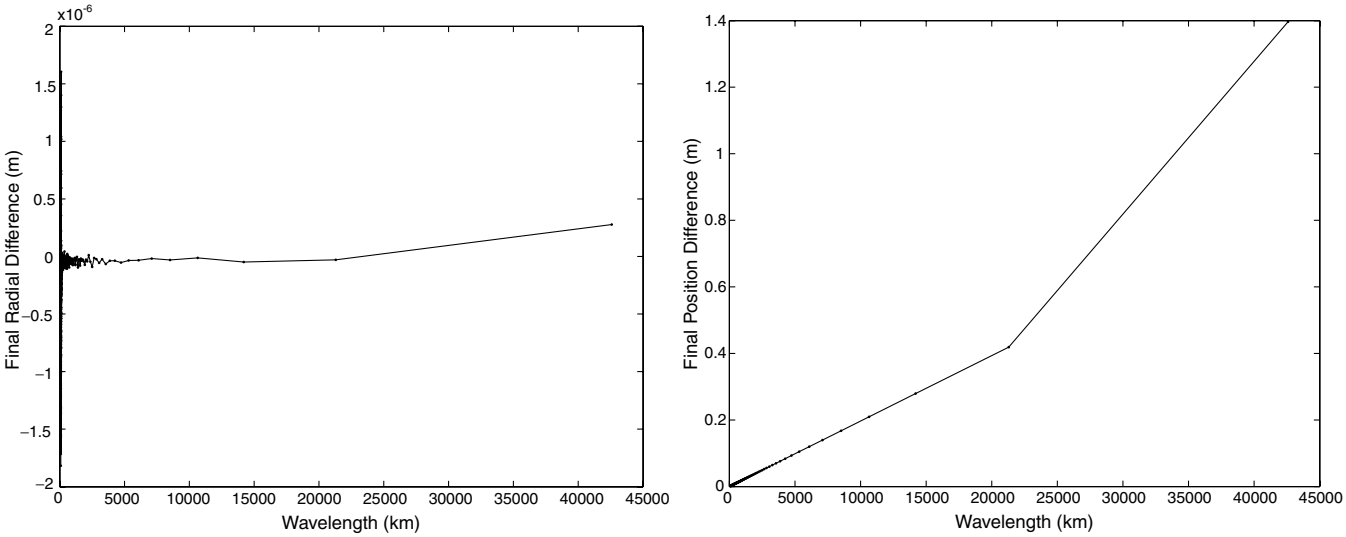

a) Radial b) Total

Fig. 6 Final orbit differences from nominal orbit as a function of density perturbation wavelengths. These trajectories were integrated for one complete orbital period.

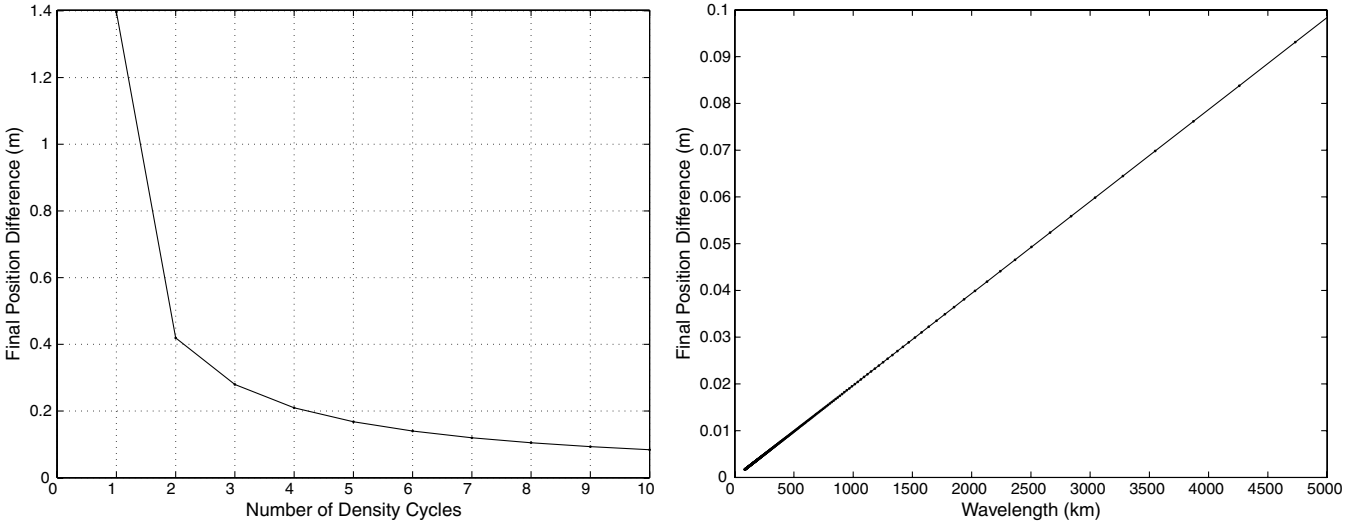

a) Position difference vs cycles **b) Total difference (close-up view)**

Fig. 7 Position difference as a function of the number of cycles and a closer view of Fig. 6b.

method would be to use an amplitude equal to the amplitude of the sine wave. It was felt, though, that a truer comparison could be obtained by choosing an amplitude that gave the same impulse or integrated ΔV over half a period of the density cycle. This value was obtained by solving Eq. (10) and plugging the solution into Eq. (11) to solve for the constant acceleration that would result in the same ΔV. Equation (1) was used to compute the density that would then result in the given acceleration. This density was then specified as the amplitude of the density perturbation for the step function. For the case in which the sine wave density amplitude was 25% of the nominal density, the acceleration obtained was approximately -3.622×10^{-8} m/s^2, which gave an amplitude for the step function of approximately 4.464×10^{-13} kg/m^3.

The step function results equivalent to the sine wave function results in Fig. 5 are given in Fig. 8. Comparing the sine wave and step function results reveals only minor differences, primarily in the magnitude of the position differences. For example, the maximum in-track difference for the sine wave case was approximately 1.4 m, and the maximum value for the step function case was 1.29 m. The fact that similar results were obtained for such different function shapes indicates that, at least for a first approximation in further studies, either function may be used. This statement may be further tested with yet another function in the form of multiple impulsive ΔV along the trajectory.

C. Impulsive ΔV

The multiple impulsive ΔV were computed by integrating the accumulated ΔV from the first half of the sine wave. This ΔV was then applied with and against the direction of motion of the spacecraft corresponding to the peaks and dips of the sine wave function. For example, in the one cycle per orbit case, a ΔV was applied against the direction of motion of the spacecraft at one-quarter of the orbital period, and then the same ΔV was applied with the velocity vector at three-quarters of an orbital period. Once again, although the position difference curves are a little more dissimilar, comparisons of the sine wave and step function cases reveal minimal differences in the final position differences. From these results in Fig. 9 and the comparison of all three cases in Fig. 10, it appears that the sine wave, step function, and impulsive ΔV cases are similar enough that the remainder of this portion of the study will use the sine wave function.

D. Negative Sine Wave

One question that may arise is whether the sign of the sine wave function has an effect on the result. A test run was done to investigate this possibility. As might be expected, the final in-track differences were the same in magnitude but in the negative direction.

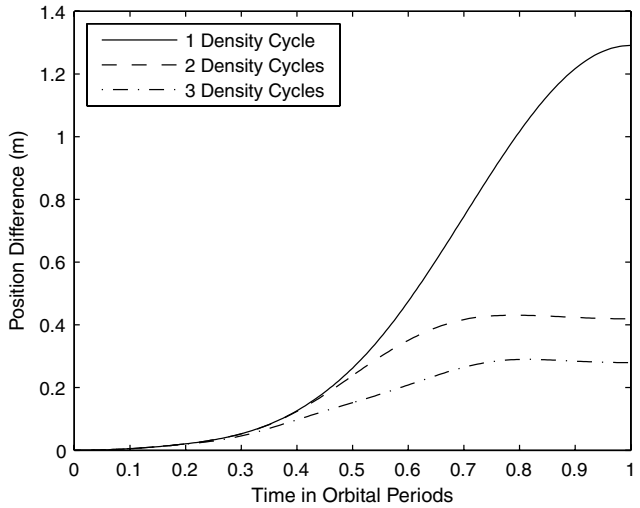

Fig. 8 Total position difference from the nominal orbit over time. The position difference was dominated by the in-track differences as expected. The integration period was for one complete orbital period with one, two, and three step function density cycles.

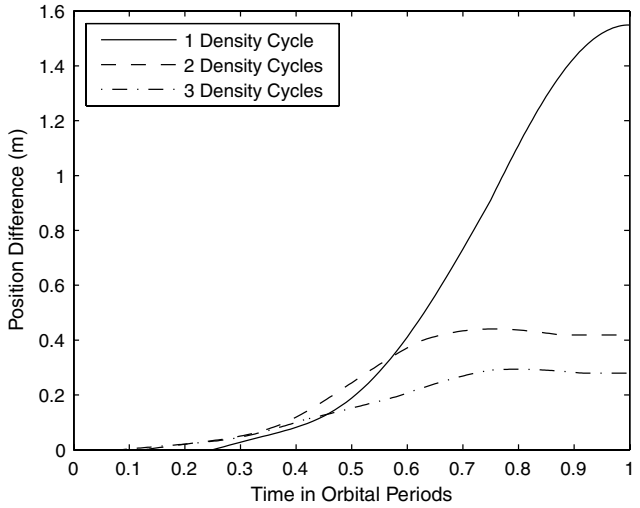

Fig. 9 Total position difference from the nominal orbit over time. The position difference was dominated by the in-track differences as expected. The integration period was for one complete orbital period using impulsive ΔV with one, two, and three cycles.

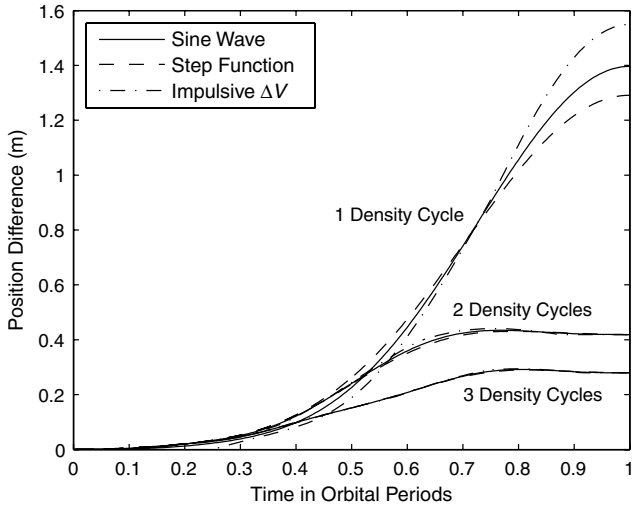

Fig. 10 Summary of the orbit differences from the nominal orbit for each function over one orbital period.

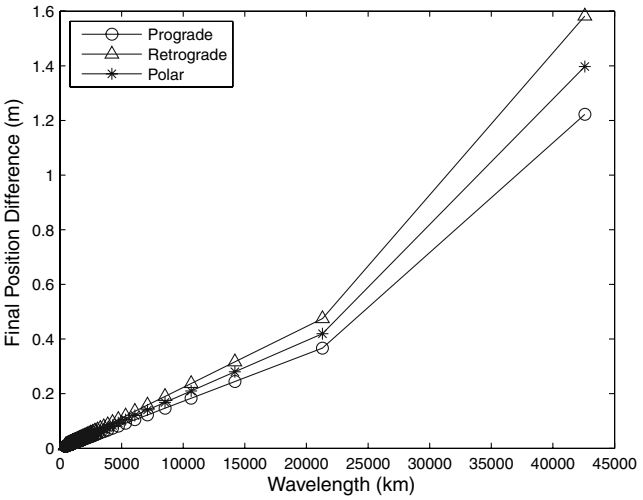

Fig. 11 Final orbit differences from the nominal orbit as a function of the wavelength of the density cycles. These results were obtained for the spacecraft integrated for one period in prograde, retrograde, and polar orbits. The total position differences are dominated by the in-track differences. The cross-track differences for the pro- and retrograde cases are zero, and the cross-track difference for the polar case (not shown) attained a maximum of approximately 4 mm. The radial differences were small enough to be considered insignificant.

E. Integration Around a Rotating Earth

The results shown so far have neglected the rotation of the Earth for simplicity and also because many of the orbits of interest, such as CHAMP, are close to polar orbits. Another interesting possibility, though, is to begin to include the rotation of the Earth in the results and determine whether it has a significant effect on the orbits. For this portion of the study, a rotation of approximately 7.292116×10^{-5} rad/s was used. The trajectories were again integrated for one period, and the rotation was included in the velocity calculation. For simplicity, the sine wave perturbed atmosphere was computed in inertial space so that one complete period would correspond to an integer number of density cycles. In other words, when the spacecraft completed one period in inertial space, it returned back to the beginning of the density cycle. The velocity of the atmosphere due to the rotating Earth was still included in the drag computations, though.

1. Equatorial Orbit (Pro- and Retrograde)

The results for an equatorial prograde orbit are shown along with those for the retrograde and polar orbits in Fig. 11. In each of these cases, the rotating atmosphere was included in the calculation with the density cycle attached to the inertial frame to ensure an integer number of density cycles. Examining the figure and comparing it with the results for the sine wave atmosphere with no rotation in Fig. 6 reveals a slight change in the magnitude of the total and in-track differences. For this prograde orbit, the differences are generally slightly less.

A similar study was done for a retrograde orbit, and the results are also given in Fig. 11. As might be expected the in-track and total differences are slightly larger than the original case without Earth rotation included.

2. Polar Orbit

The results for a polar orbit are also included for comparison in Fig. 11. The differences from the case without the rotating Earth are slight, and the final position differences fall between the pro- and retrograde cases. Note that now there is a slight cross-track difference with a maximum value of approximately 4 mm between the two orbits.

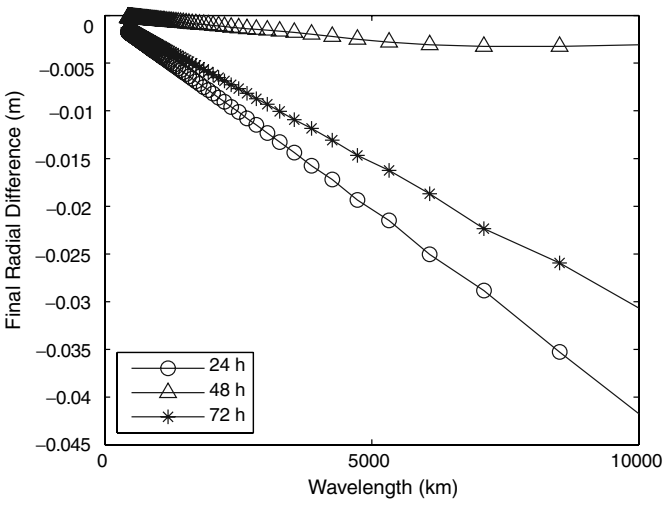

a)

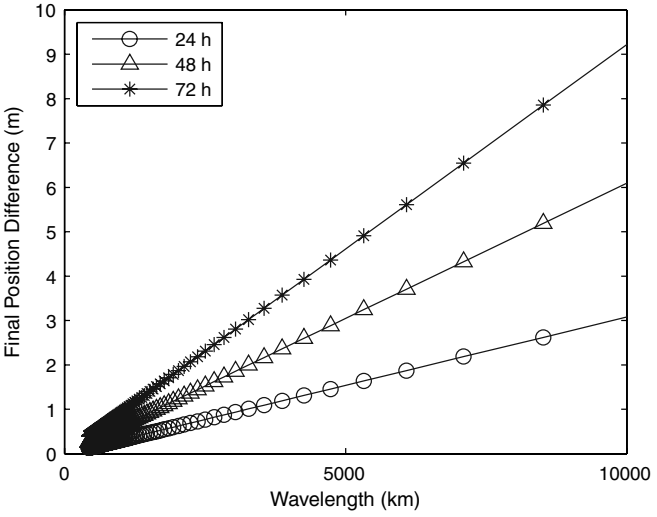

b)

Fig. 12 Orbit differences after 24, 48, and 72 h using a sine wave and focusing on shorter wavelengths. Note that the total orbit differences are dominated by the in-track differences.

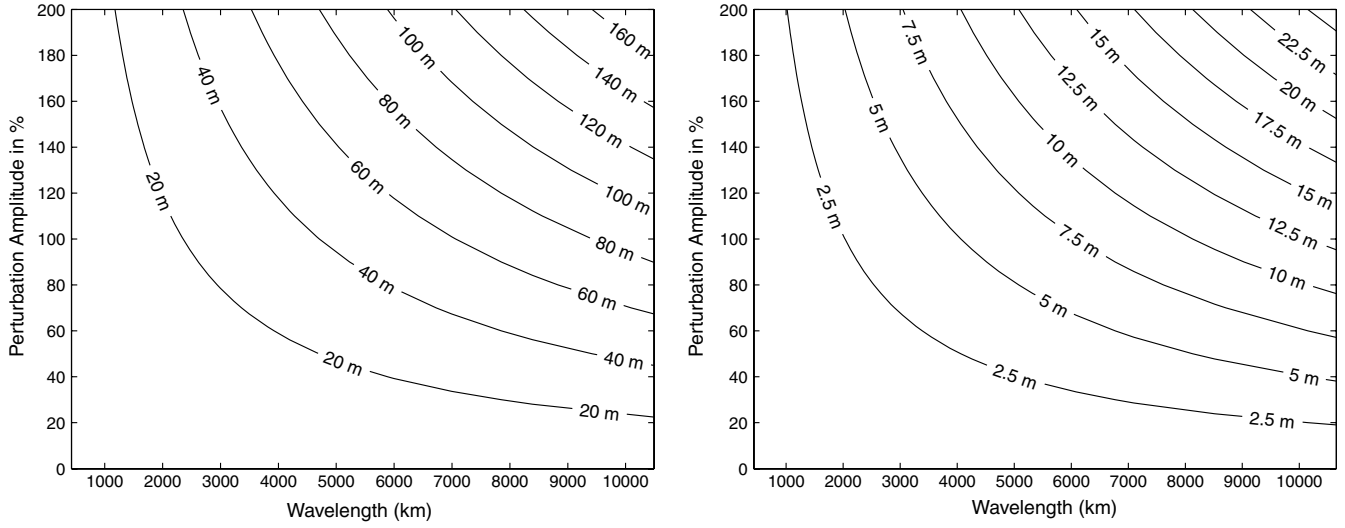

a) b)

Fig. 13 Orbit position differences after 24 h for circular orbits with varying amplitudes for the density sine waves: a) 300 km, and b) 400 km.

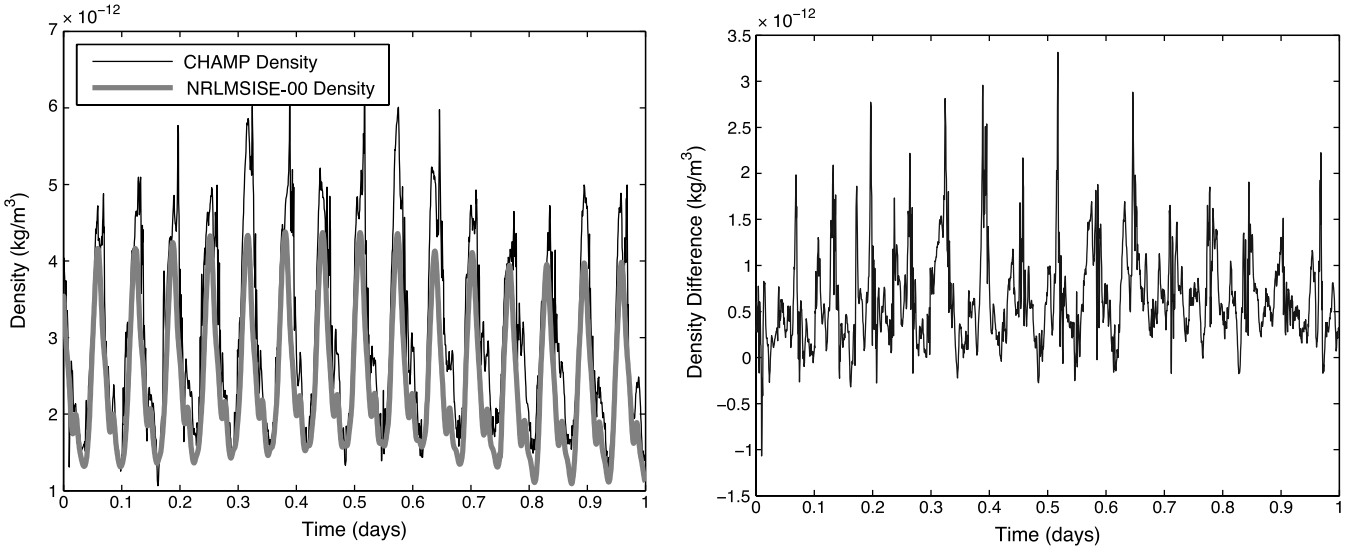

a) Densities **b) Actual - model density**

Fig. 14 Measured and modeled densities along the CHAMP orbit for day 175 of 2003.

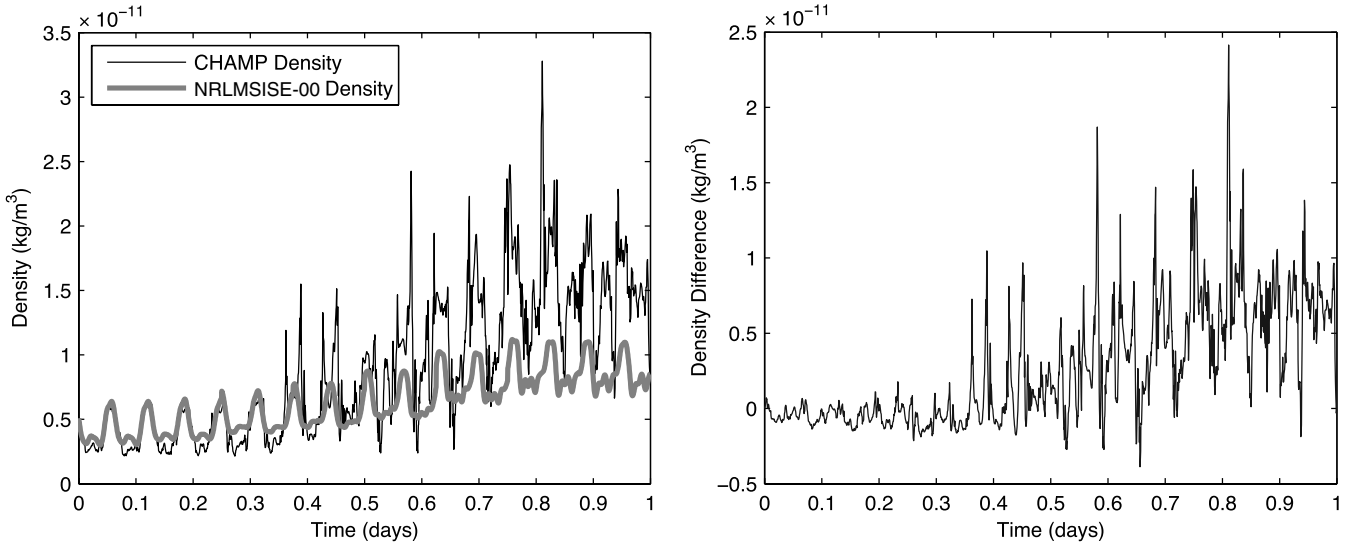

a) Densities **b) Actual - model density**

Fig. 15 Measured and modeled densities along the CHAMP orbit for day 324 of 2003.

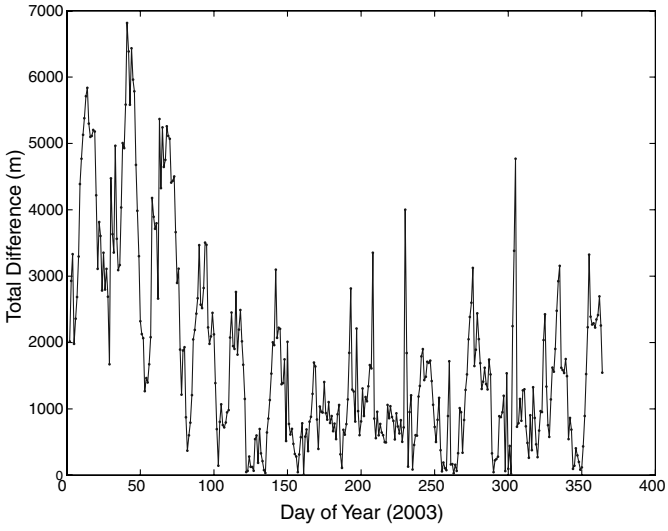

a) Total

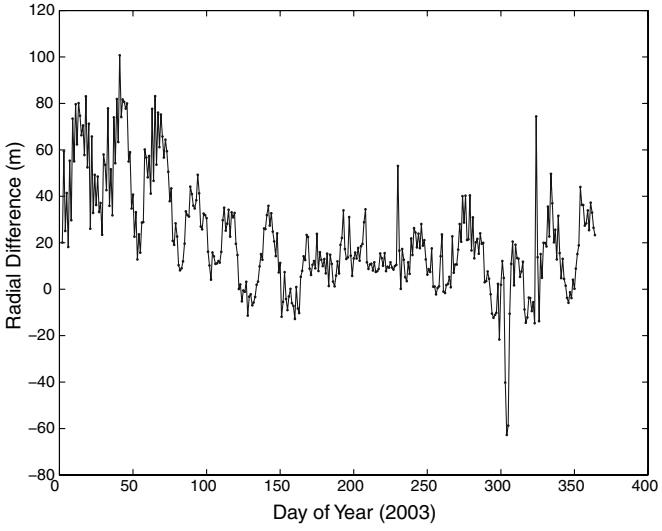

b) Radial

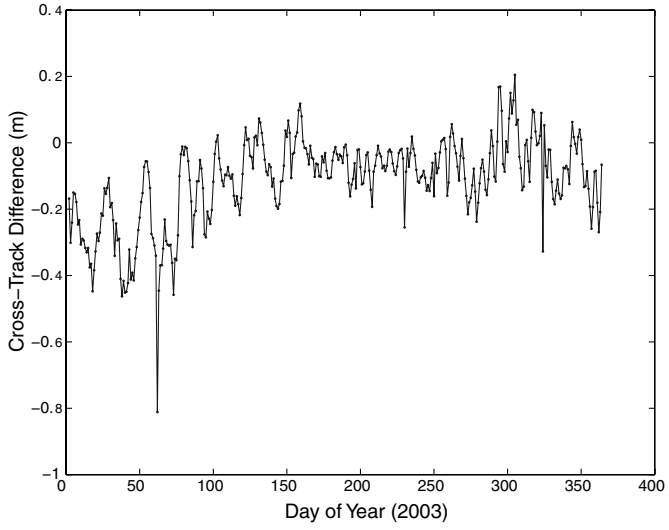

c) Cross-Track

Fig. 16 Orbit differences for 2003 using a 24 h integration. The difference is computed between an orbit integrated using the NRLMSISE-00 model densities and an orbit integrated using CHAMP's measured densities mapped to 400 km.

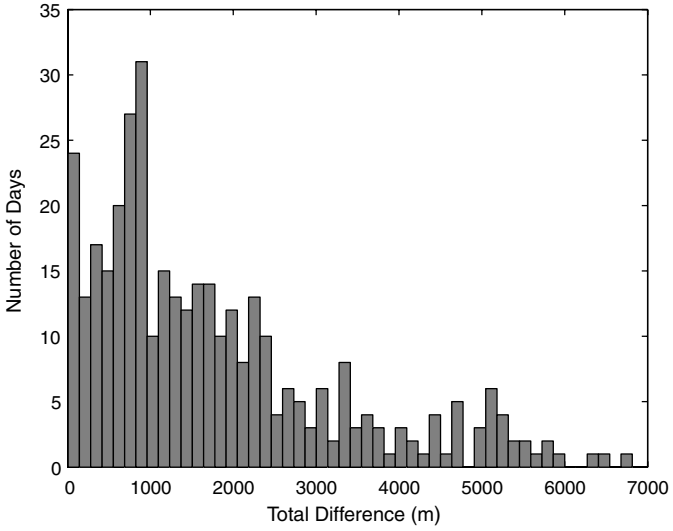

a) 2003 (from Fig. 16a)

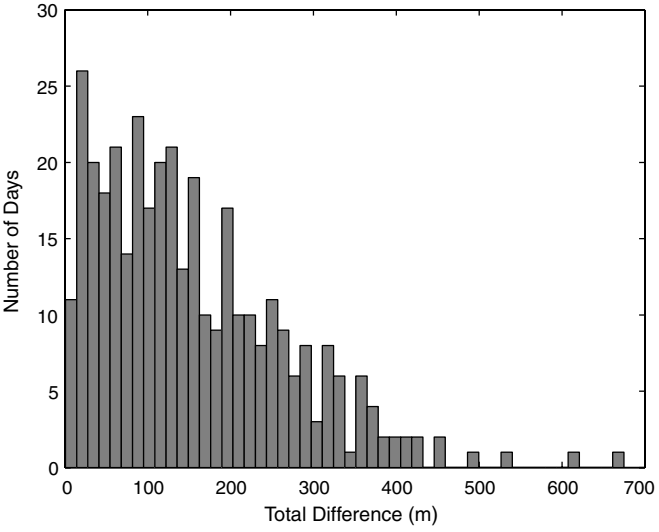

b) 2007

Fig. 17 Histograms of the total orbit differences for each year.

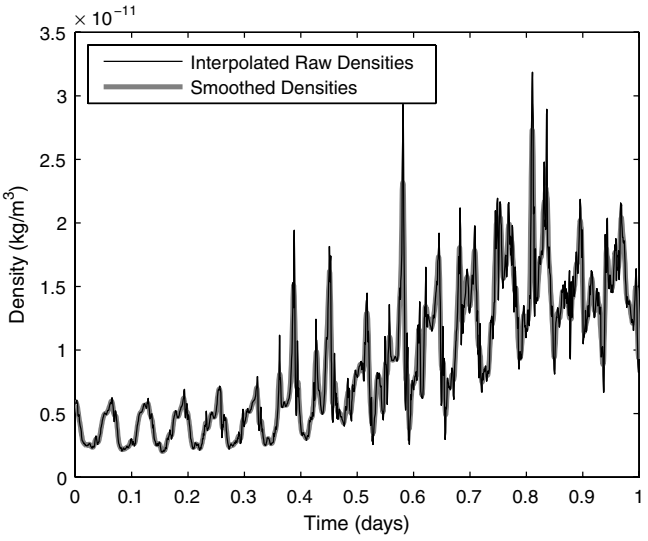

a) 6 min interval

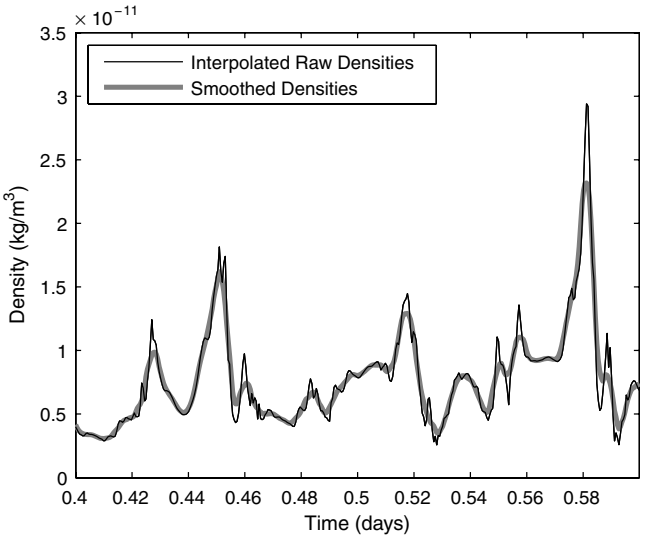

b) 6 min interval (closer view)

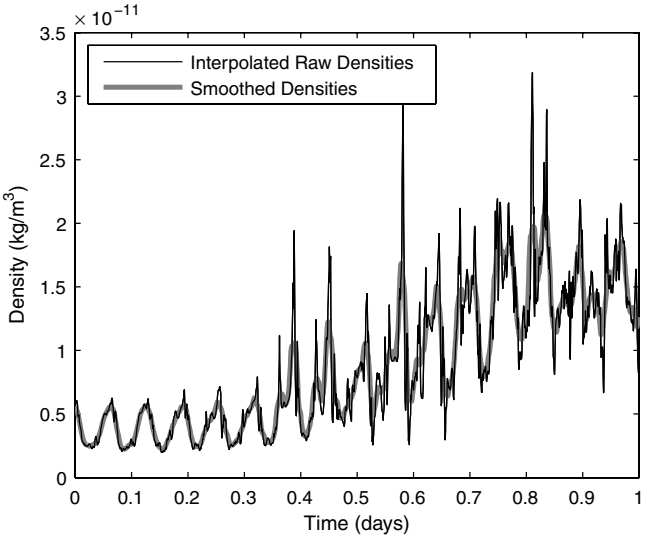

c) 18 min interval

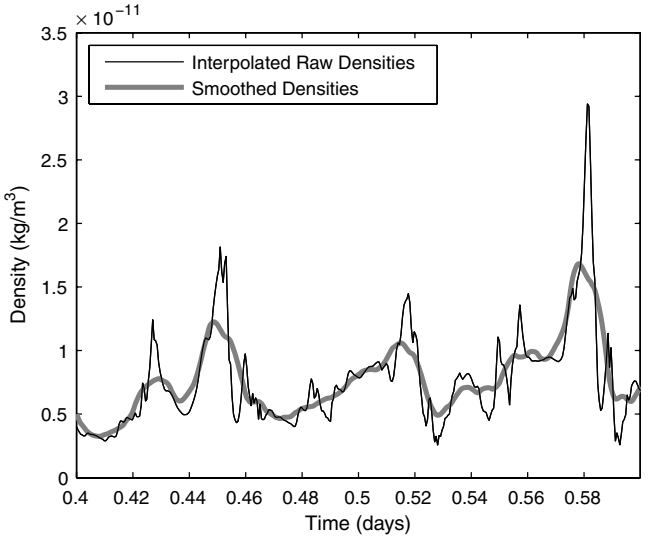

d) 18 min interval (closer view)

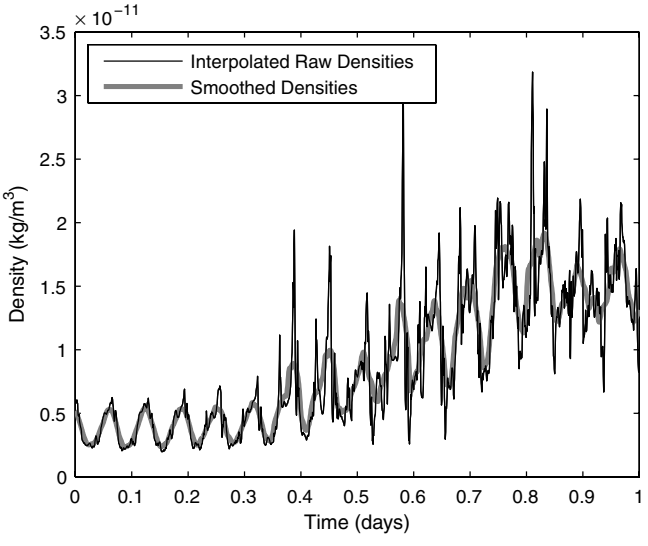

e) 30 min interval

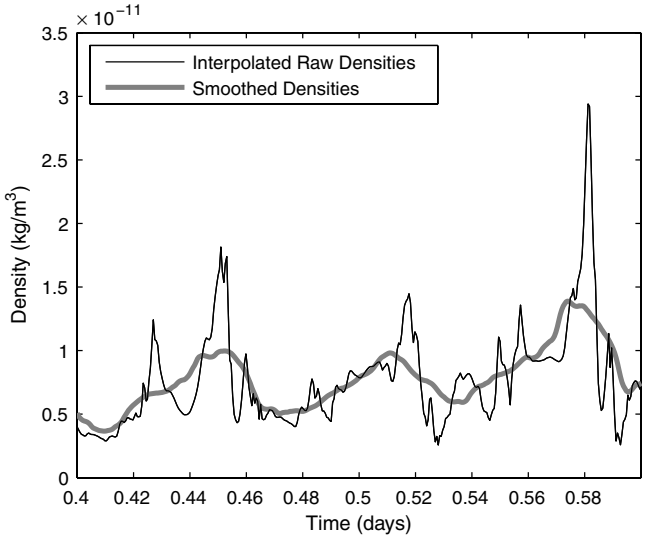

f) 30 min interval (closer view)

Fig. 18 Interpolated raw and smoothed densities over 24 h averaged using different time intervals. These plots were computed for day 324 of 2003.

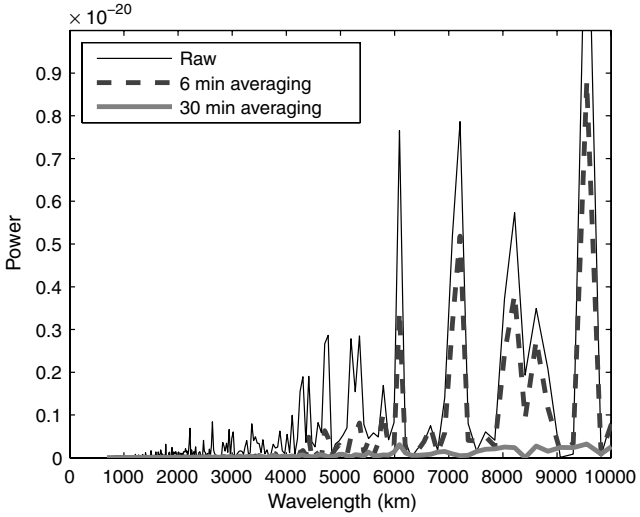

Fig. 19 Power spectral densities for the raw CHAMP data, the 6 min case, and the 30 min case.

F. Longer Integration Times

Although the plots so far have given an indication of the relative effects of different horizontal wavelengths by looking at shorter integration times, it is more relevant to look at the one-, two-, and three-day time scales typically of concern for orbit predictions. The results from these types of integrations over the time scales of interest are shown in Fig. 12.

Comparing the results for the different integration times reveals that the maximum total difference over this span increases approximately 3 m for each additional day. The values are below those that would be of concern for the U.S. Air Force, but they are not negligible. One possibility is that the effects of each of these wavelengths could be cumulative, and if they are not taken into account, the total effect could be greater. This question will be examined in more detail through analysis of the CHAMP data.

G. Varying Additional Parameters

It is worth taking some time to examine the effects of varying some of the basic parameters chosen for this study. Quantifying some of these effects should give an idea of how some of the conclusions obtained in this paper would change given different conditions. One of the studies performed was to examine the effect of changing the

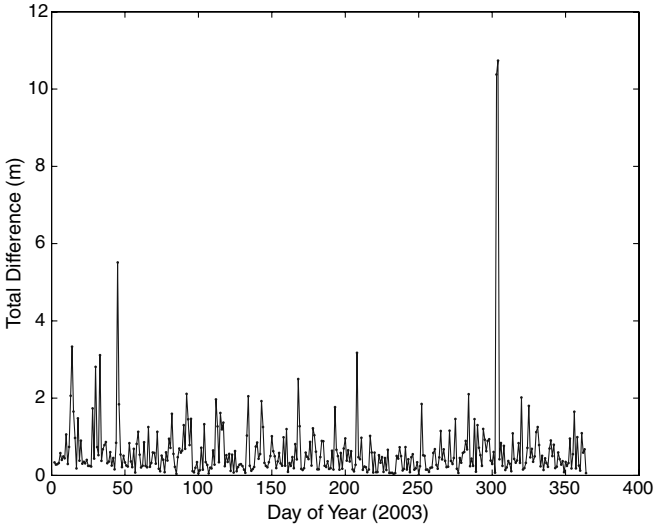

a) Total

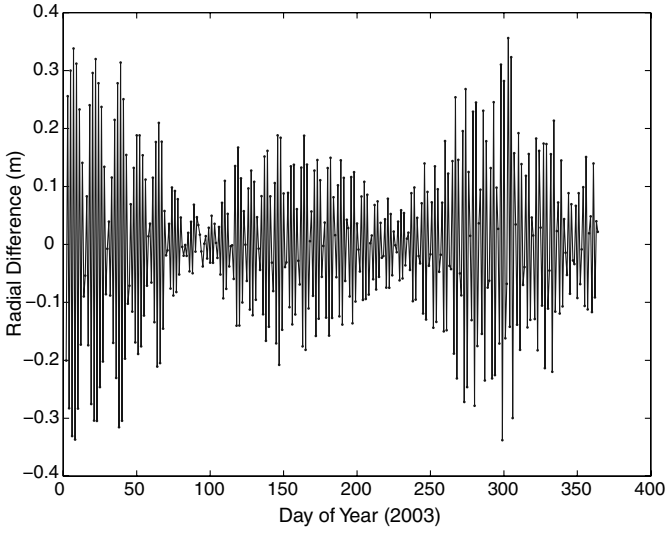

b) Radial

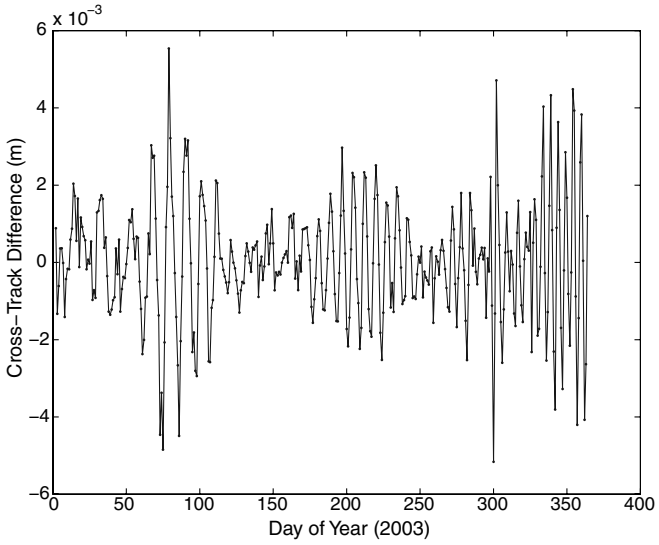

c) Cross-Track

Fig. 20 Orbit differences between the case using the actual densities and the case using the smoothed densities for 2003 using a 24 h integration and 6 min averaging interval.

Table 2 Orbit differences at the end of a 24 h integration on day 324 of 2003

Integration time, h	Averaging time, min	Radial diff., m	In-track diff., m	Cross-track diff., m	Total diff., m	Energy diff., m^2/s^2
24	6	0.16	−0.69	0.00030	0.71	0.050
24	18	1.23	−4.93	0.0029	5.08	−0.046
24	30	3.16	−9.69	0.0092	10.19	0.073
72	6	−0.23	−2.13	−0.0072	2.15	−0.017
72	18	−1.74	−15.15	−0.052	15.25	−0.043
72	30	−4.56	−29.84	−0.12	30.19	0.074

amplitude of the density sine wave and then to compare the differences for orbits of different altitudes. The results from this study are given in Fig. 13. These results can be placed within the context of the previous analysis by examining the results for the 400 km case. Increasing the density sine wave amplitude has a noticeable effect, as might be expected. For example, at the 7000 km wavelength, the position difference increases from approximately 2.5 m at a 25% amplitude to over 15 m at a 200% amplitude. Varying the altitude of the circular orbit to 300 km results in a little less than a factor of 10 increase in the position differences. Further studies showed that continuing down to 200 km actually gives an increase of approximately 100 over the 400 km case. Likewise, increasing the altitude to 600 km results in an order of magnitude decrease from the 400 km case. At 800 km, the maximum differences are less than 10 cm. An additional study examining the effects of varying the drag coefficient found that the position differences varied linearly with the drag coefficient. It is expected that this information may be used as a general guide to apply the results in this paper to new cases.

V. Density Model vs Measured Data

One of the basic questions of the current research program is related to how accurately current density models allow the prediction of orbits. This question is analyzed here in a straightforward way by comparing the orbit predictions using the model's density profiles and densities derived from the CHAMP accelerometer obtained from

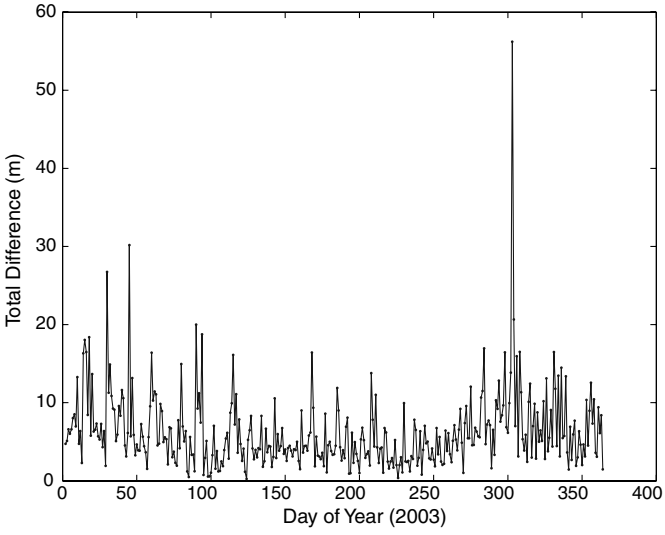

a) Total

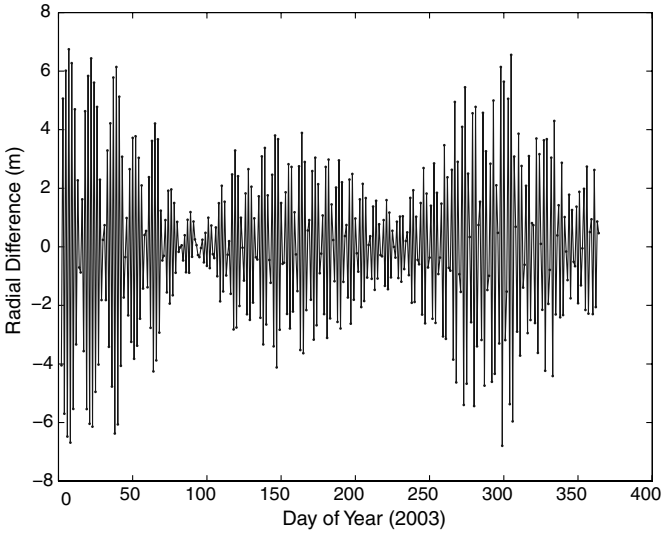

b) Radial

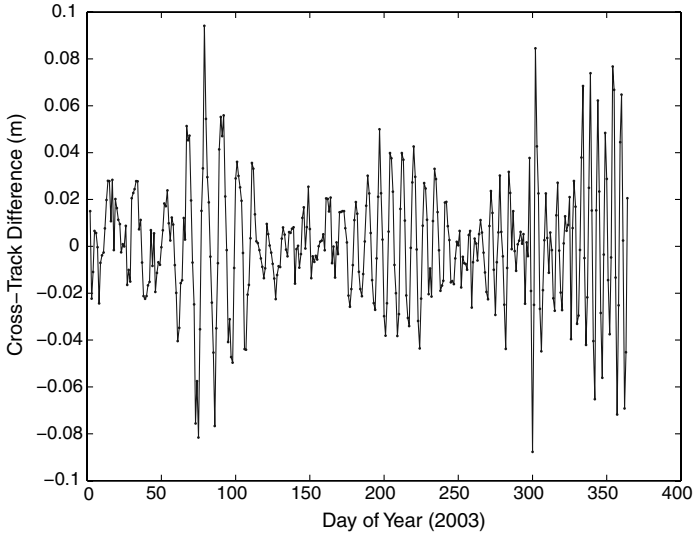

c) Cross-Track

Fig. 21 Orbit differences between the case using the actual densities and the case using the smoothed densities for 2003 using a 24 h integration and 30 min averaging interval.

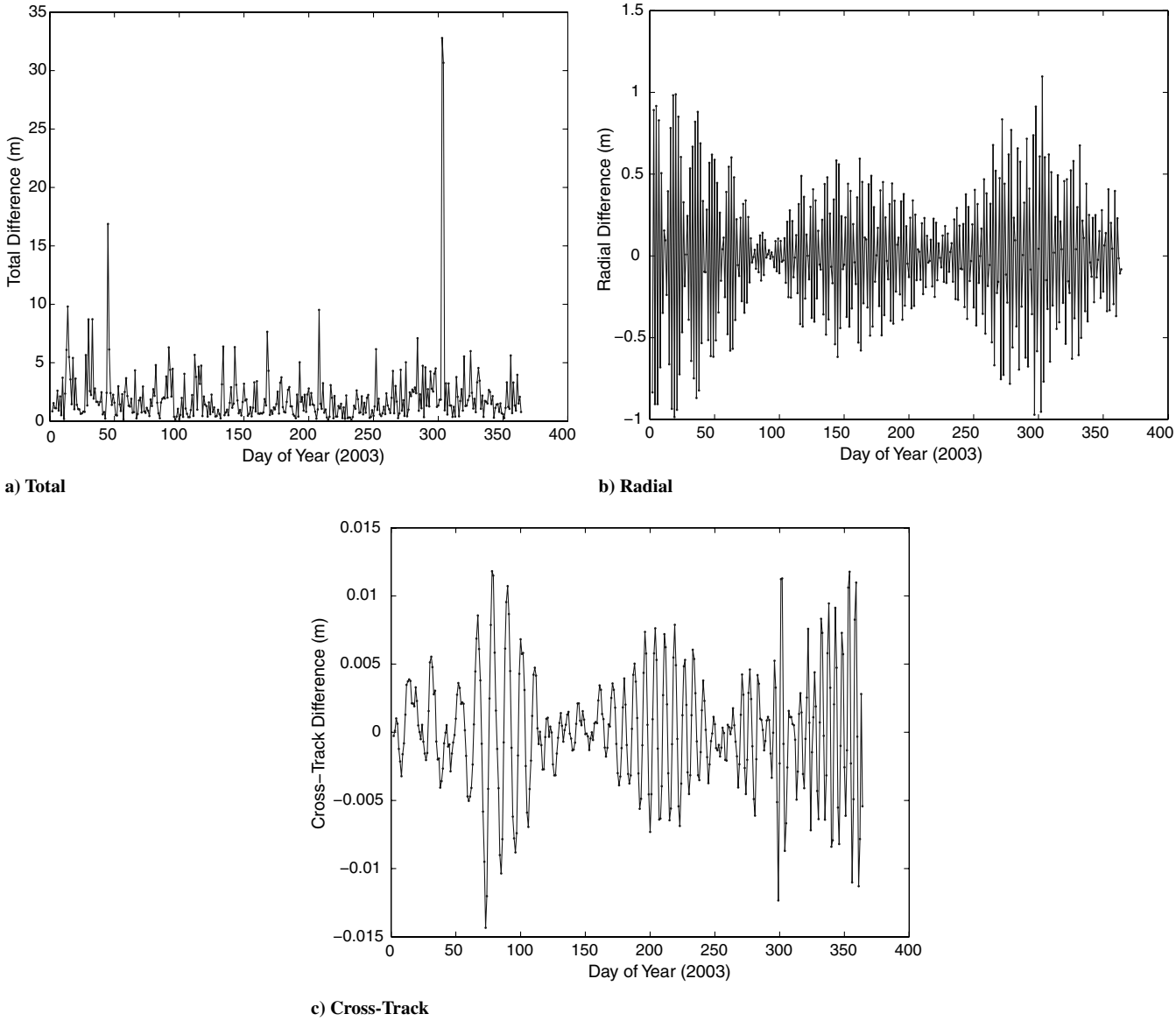

a) Total **b) Radial** **c) Cross-Track**

Fig. 22 Orbit differences between the case using the actual densities and the case using the smoothed densities for 2003 using a 72 h integration and 6 min averaging interval.

Sutton's website.[§] For the purposes of this study, these densities derived from CHAMP's accelerometer are assumed to be the actual density profile. The model used here was the NRLMSISE-00 model. Remember that CHAMP's initial altitude was 454 km, and its altitude varied from an approximate high of 438 km in 2003 to an approximate low of 337 km in 2007.

The differences in the actual densities are easily seen by looking at the plots of the measured and modeled densities along the CHAMP orbit for two days of interest in 2003. These plots are given in Figs. 14 and 15 for days 175 and 324 of 2003, respectively. Both the measured and modeled data are taken directly from the CHAMP data set described earlier. (The modeled densities are provided in the data set for CHAMP's current location.)

A comparison was made by integrating one orbit with the measured densities and one orbit with the modeled densities from the same initial conditions over a period of 1 day. The usual 400 km circular orbit was used in this simulation. The NRLMSISE-00 densities at 400 km were not provided in the data set obtained from Sutton's website, and so the accelerometer derived densities were scaled to 400 km using the ratio of NRLMSISE-00 densities between the actual altitude and 400 km.

The resulting differences over 2003, an active year, are shown after integrating for 1 day for each day of the year in Fig. 16. From these plots, it can be seen that there are, at times, significant differences after a 24 h period. The primary differences are in the in-track direction, as would be expected. The maximum difference is 6817 m, and the minimum difference is approximately 7 m. The mean is a relatively large value of 1785 m. The histogram in Fig. 17a reveals that a significant number of these cases fall in the 1–2 km range. Errors in this range are obviously of concern.

The performance of the density model improved dramatically for the quieter year of 2007. The total orbit differences computed in Fig. 17b are on the order of 100 to several hundred meters. These values are more in line with the requirements and expectations of the U.S. Air Force for their orbit predictions.

VI. Predictions with Measured and Smoothed Challenging Minisatellite Payload Data

Although the model densities have been found to introduce a significant error into the orbit prediction, it remains to be seen which parts of the model are most responsible for this error. This study

[§]Data available online at http://sisko.colorado.edu/sutton/ [retrieved 1 July 2008].

focuses on the horizontal scales that are of most importance, and so a method was selected to help reduce the effect of certain horizontal scales and thereby evaluate their importance.

This method involved smoothing the actual CHAMP data by averaging it over specified time intervals. The data were generally given at time intervals of 45 s, and so averages over some integer multiple of these data points were selected. The two time intervals that were primarily used were the 6 and 30 min time intervals. With an orbital speed of approximately 7668.56 m/s for the 400 km orbit, this gives corresponding distances of 2760.68 and 13,803.41 km, respectively. These two distances are adequate to smooth out the approximate 1000 and 8000 km (roughly 10 and 70° of latitude, respectively) scales that Sutton found to be of importance in his dissertation [11].

The densities used in the integration were those densities mapped to 400 km using the NRLMSISE-00 model as provided in the CHAMP data. The orbit in each case was a 400 km circular orbit. The procedure involved integrating one orbit with the original CHAMP densities mapped to 400 km and then integrating another orbit from the same initial conditions with a smoothed version of the densities.

To obtain an idea of what different levels of averaging mean to the density profile, the results from three different averaging times are shown in Fig. 18 and compared with the measured densities interpolated to the same time intervals. Occasionally the measured densities were given at uneven time intervals, and so interpolation was used to insure that densities were available every 45 s. The power spectral densities are shown for the raw data, the 6 min case, and the 30 min case in Fig. 19. The plot confirms that the power has been reduced at the shorter wavelengths for the 6 min case, and the 30 min case has reduced power through 10,000 km.

Several point comparisons were made using these density profiles for day 324 of 2003. In each comparison, orbits were integrated from the same initial conditions using the measured and smoothed densities, respectively. The differences in the orbits at the end of the integration were compared and tabulated in Table 2. From these results it can be seen that the errors increased substantially with each increase in the averaging time interval. For the 24 h case, increasing the averaging interval from 6 to 30 min results in an increase in the final orbit error of over one magnitude. This result might be expected from the fact that the smoothed density at the 30 min level demonstrates significantly more noticeable deviations from the measured data than at the 6 min level. The 72 h cases with an integration three times as long appear to result in about three times the error in each case. These errors are still below values that might necessarily be of concern to the U.S. Air Force, but it is worth remembering that many other factors will contribute to the total error, and these values are reaching the level that must be taken into account for orbit predictions.

Although an analysis of 1 day of data is insightful, it is worth examining a whole year of data to obtain a more complete picture. In

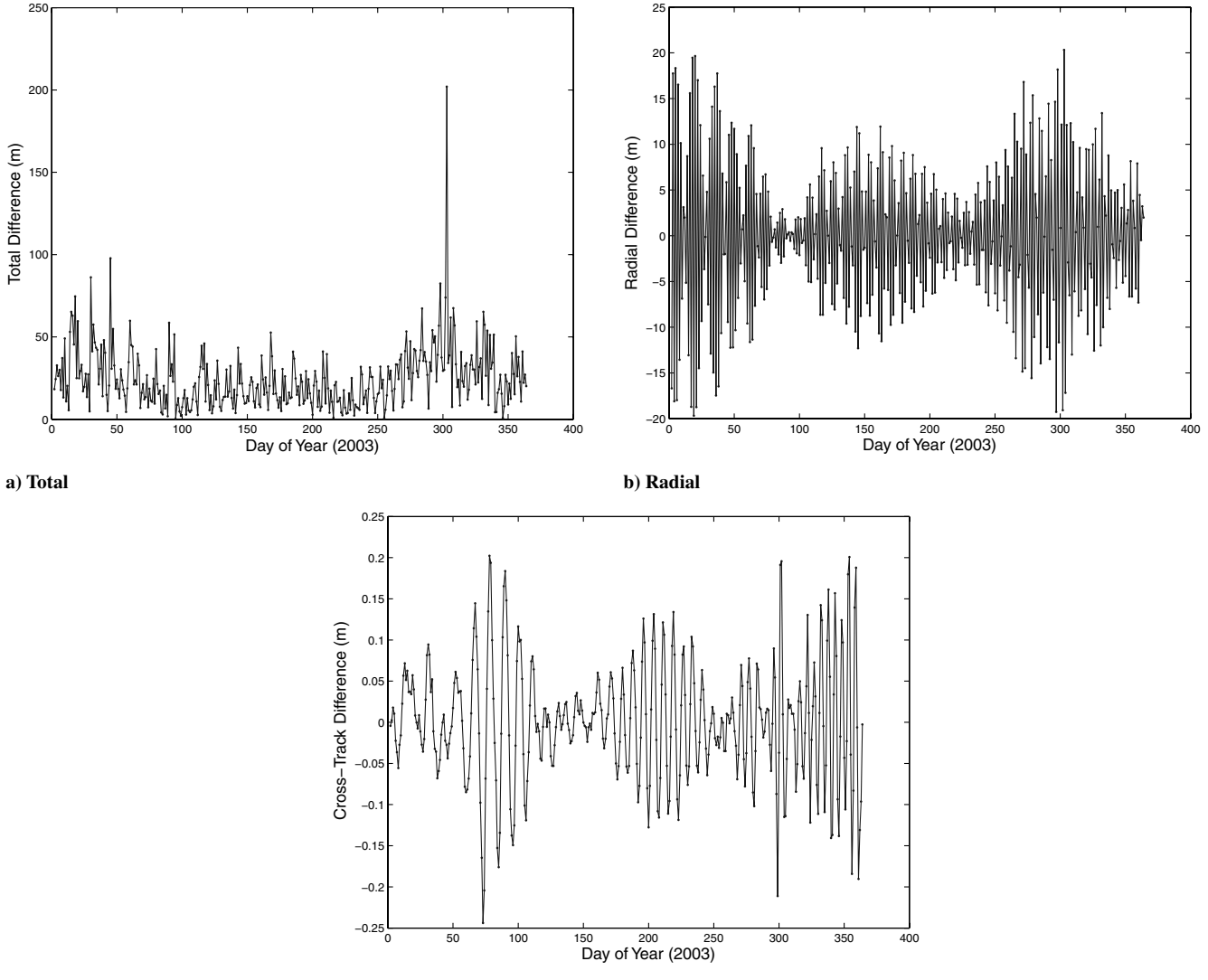

a) Total **b) Radial**

c) Cross-Track

Fig. 23 Orbit differences between the case using the actual densities and the case using the smoothed densities for 2003 using a 72 h integration and 30 min averaging interval.

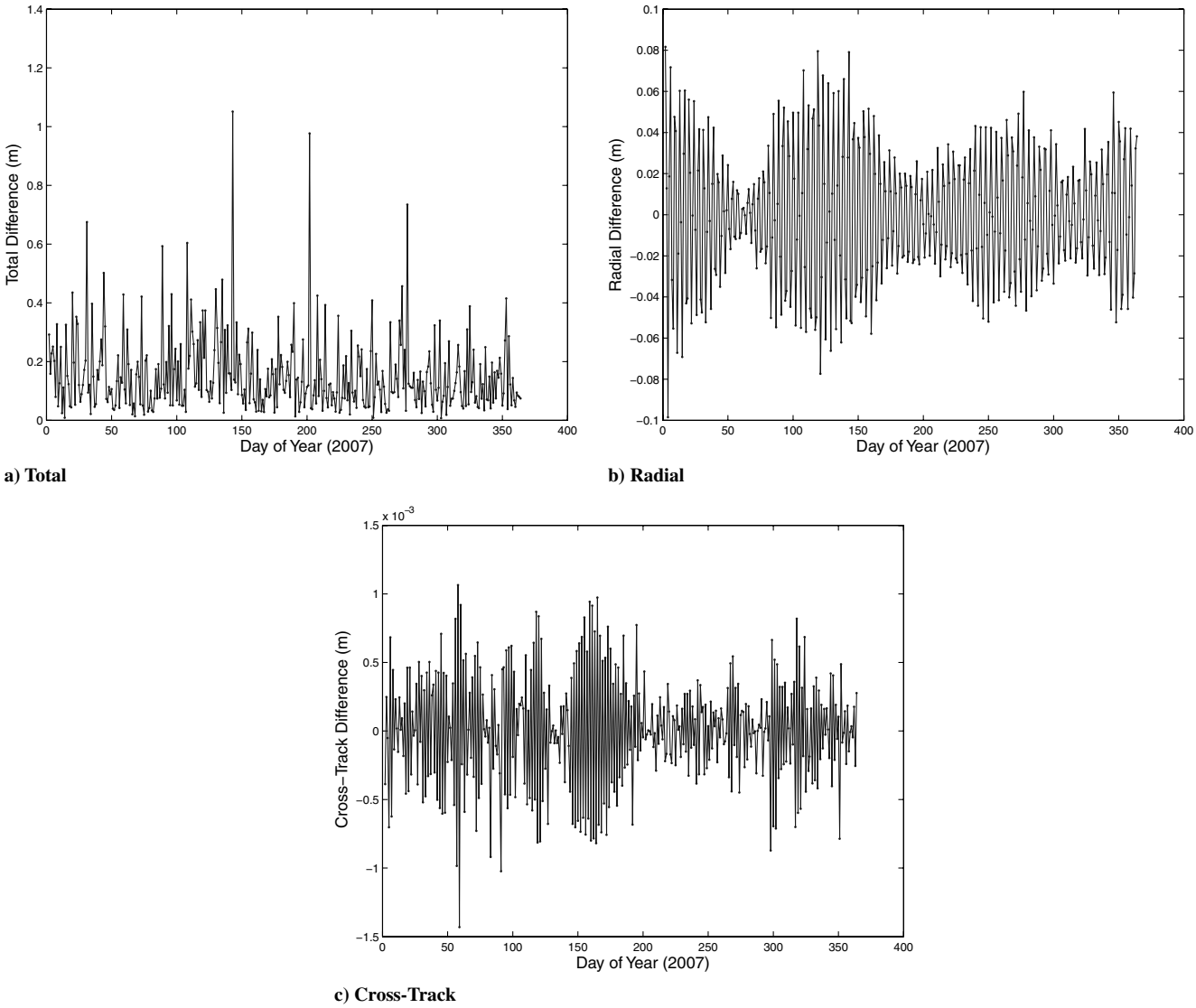

Fig. 24 Orbit differences between the case using the actual densities and the case using the smoothed densities for 2007 using a 24 h integration and 6 min averaging interval.

the following analysis, the orbit differences for all of 2003 (an active year) and 2007 (a quiet year) are examined for the 6 and 30 min averaging time intervals. Figures 20 and 21 summarize the results for 2003 with a 24 h integration. The 6 min averaging interval resulted in a maximum total difference of approximately 10.7 m, a minimum of 0.019 m, and a mean of 0.63 m. Using the 30 min averaging interval made these values jump to 56.21 m for the maximum, 0.24 m for the minimum, and 6.21 m for the mean. The jump in the mean is similar to the jump observed for day 324 of 2003.

As expected, the differences jump once again when the time is increased to 72 h, as shown in Figs. 22 and 23. The mean for the 6 min case increases to 2.06 m, with maximum and minimum values of 32.79 and 0.090 m, respectively. For the 30 min case, the mean becomes 24.40 m, with maximum and minimum values of 202.07 and 0.29 m, respectively. Some of the maximum values are starting to reach the magnitude at which they would be of significant concern on their own even without taking other factors into account. However, 2003 was a particularly active year, and so it is worth examining the quieter year of 2007.

Examining the data over 2007 reveals noticeably smaller orbit differences, as shown in Figs. 24 and 25. The maximum difference for the 6 min averaging interval is 1.05 m, with a minimum of 0.0071 m and a mean of 0.15 m. With a 30 min averaging interval, the maximum is 7.60 m, with a minimum of 0.14 m and a mean of 1.79 m. These values are significantly smaller than those computed for 2003 and indicate that the amount of variability in the atmosphere may be a factor in determining how accurate the density prediction models need to be. Remember that all these values are for the given spacecraft and may vary somewhat with the actual characteristics of the spacecraft, but they give a general sense of expected results.

The total orbit differences for the two years are summarized in Fig. 26 for the worst-case 30 min averaging interval. Nearly one order of magnitude difference in the total orbit differences can be easily observed here. This result indicates on some level the importance of more accurate models when the density variability is high.

VII. Conclusions

The sensitivity of orbit predictions to density variability has been analyzed, particularly with regard to the effect of various horizontal wavelengths in the density profile. A series of simple density perturbation models revealed that the errors imposed by a single density wavelength on the chosen spacecraft were small relative to U.S. Air Force requirements, but not negligible. An analysis of orbit predictions using the NRLMSISE-00 model compared with CHAMP measured densities along a simulated two-body orbit revealed significant orbit prediction differences for 2003, whereas the results for the quieter year of 2007 were more in line with the expected values, given U.S. Air Force requirements. This indicates that there is

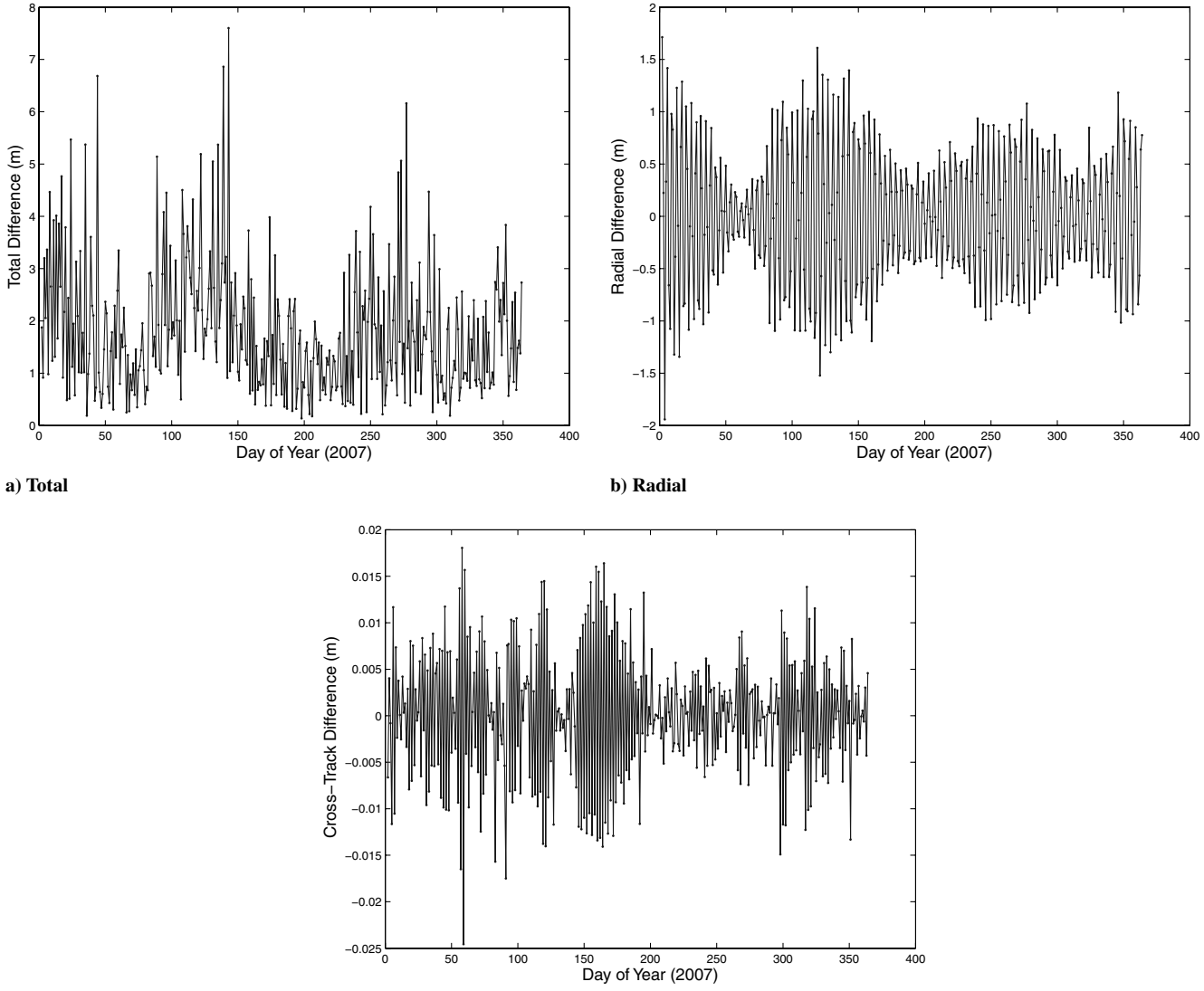

Fig. 25 Orbit differences between the case using the actual densities and the case using the smoothed densities for 2007 using a 24 h integration and 30 min averaging interval.

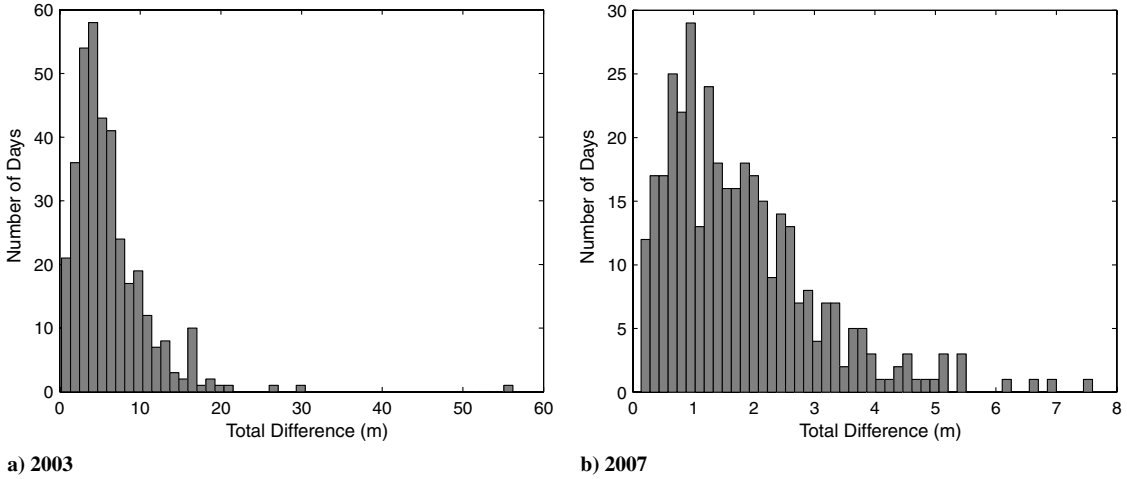

Fig. 26 Histogram comparison of the total orbit differences using a 24 h integration and 30 min averaging.

room for improvement in the model, especially with regard to more active years. It is worth noting that these results were for the CHAMP spacecraft and that eventually including additional spacecraft will be important. The included analysis using different spacecraft parameters serves as a general guide for how these results would vary for different spacecraft. Whereas the simple model attempted to isolate the effect of particular horizontal wavelengths, the next step attempted to remove the effect of a set of horizontal

wavelengths below a cutoff wavelength. It was determined that the effect of not including these wavelengths in the prediction process was significant as well as sometimes greater than the effect of a single wavelength. Errors on the order of magnitude of the U.S. Air Force requirements were introduced particularly when wavelengths on the order of 8000 km (approximately 70° of latitude) were averaged out. Errors were reduced to the order of several meters for the given spacecraft when the averaging occurred over less than approximately 10° of latitude.

Acknowledgments

This research was supported by the Multidisciplinary University Research Initiative Neutral Atmosphere Density Interdisciplinary Research program at the University of Colorado at Boulder. The authors would like to thank Bruce Bowman, Senior Astrodynamicist, U.S. Air Force Space Command, Space Analysis Center, Peterson Air Force Base, Colorado for his helpful discussions and information, especially with regard to the 24 h orbit prediction errors of significance to the U.S. Air Force. The authors would also like to thank Eric Sutton for providing the CHAMP data and atmosphere code, as well as for his insights into using them.

References

[1] Marcos, F. A., "Accuracy of Atmospheric Drag Models at Low Satellite Altitudes," *Advances in Space Research*, Vol. 10, No. 3, 1990, pp. 417–422.
doi:10.1016/0273-1177(90)90381-9

[2] Marcos, F. A., Kendra, M. J., Griffen, J., Bass, J. N., Larson, D. R., and Liu, J. J., "Precision Low Earth Orbit Determination Using Atmospheric Density Calibration," *Journal of the Astronautical Sciences*, Vol. 46, No. 4, 1998, pp. 395–409.

[3] Forbes, J. M., "Low-Altitude Satellite Ephemeris Prediction," U.S. Air Force Cambridge Research Lab. Rept. 72-0428, July 1972.

[4] Jacchia, L. G., "Thermospheric Temperature, Density, and Composition: New Models," Smithsonian Astrophysical Observatory Rept. 375, Cambridge, MA, 1977.

[5] Forbes, J. M., "Wave Structures in Lower Thermosphere Density from Satellite Electrostatic Triaxial Accelerometer Measurements," *Journal of Geophysical Research*, Vol. 100, No. A8, Aug. 1995, pp. 14693–14701.
doi:10.1029/95JA00065

[6] Rhoden, E. A., Forbes, J. M., and Marcos, F. A., "The Influence of Geomagnetic and Solar Variabilities on Lower Thermosphere Density," *Journal of Atmospheric and Solar-Terrestrial Physics*, Vol. 62, 2000, pp. 999–1013.
doi:10.1016/S1364-6826(00)00066-3

[7] Georges, T. M., "HF Doppler Studies of Travelling Ionospheric Disturbances," *Journal of Atmospheric and Terrestrial Physics*, Vol. 30, 1968, pp. 735–746.
doi:10.1016/S0021-9169(68)80029-7

[8] Sutton, E. K., Forbes, J. M., Nerem, R. S., and Woods, T. N., "Neutral Density Response to the Solar Flares of October and November, 2003," *Geophysical Research Letters*, Vol. 33, 2006, pp. L22101.1–L22101.5.
doi:10.1029/2006GL027737

[9] Sutton, E. K., Nerem, R. S., and Forbes, J. M., "Atmospheric Density and Wind Measurements Deduced from Accelerometer Data," *Journal of Spacecraft and Rockets*, Vol. 44, No. 6, Nov.–Dec. 2007, pp. 1210–1219.
doi:10.2514/1.28641

[10] Sutton, E. K., Forbes, J. M., and Knipp, D. J., "Rapid Response of the Thermosphere to Variations in Joule Heating," *Geophysical Research Letters*, Vol. 114, 2009, p. A04319.
doi:10.1029/2008JA013667

[11] Sutton, E. K., "Effects of Solar Disturbances on the Thermosphere Densities and Winds from CHAMP and GRACE Accelerometer Measurements," Ph.D. Dissertation, Univ. of Colorado, Boulder, CO, May 2008.

[12] Bowman, B. R., "True Satellite Ballistic Coefficient Determination for HASDM," AIAA Paper 2002-4887, Aug. 2002.

[13] Bowman, B. R., and Storz, M. F., "Time Series Analysis of HASDM Thermospheric Temperature and Density Corrections," AIAA Paper 2002-4890, Aug. 2002.

[14] Bowman, B. R., Marcos, F. A., and Kendra, M. J., "A Method for Computing Accurate Daily Atmospheric Density Values from Satellite Drag Data," *Advances in the Astronautical Sciences*, Vol. 119, Feb. 2004, pp. 1117–1134.

[15] Bowman, B. R., "The Semiannual Thermospheric Density Variation from 1970 to 2002 Between 200–1100 km," *Advances in the Astronautical Sciences*, Vol. 119, Feb. 2004, pp. 1135–1154.

[16] Bowman, B. R., "The Semiannual Thermospheric Density Variation at Altitudes of 160–300 km," *Advances in the Astronautical Sciences*, Vol. 123, Aug. 2005, pp. 49–58.

[17] Bowman, B. R., and Kenneth, M., "Drag Coefficient Variability at 175–500 km from the Orbit Decay Analyses of Spheres," *Advances in the Astronautical Sciences*, Vol. 123, Aug. 2005, pp. 117–136.

[18] Casali, S. J., and Barker, W. N., "Dynamic Calibration Atmosphere (DCA) for the High Accuracy Satellite Drag Model (HASDM)," AIAA Paper 2002-4888, Aug. 2002.

[19] Storz, M. F., Bowman, B. R., Branson, M. J. I., Casali, S. J., and Tobiska, W. K., "High Accuracy Satellite Drag Model (HASDM)," *Advances in Space Research*, Vol. 36, No. 12, 2005, pp. 2497–2505.
doi:10.1016/j.asr.2004.02.020

[20] Lichten, S. M., Bar-Sever, Y. E., Bertiger, W. I., Heflin, M., Hurst, K., Muellerschoen, R. J., Wu, S. C., Yunck, T. P., and Zumberge, J., "GIPSY-OASIS II: A High Precision GPS Data Processing System and General Satellite Orbit Analysis Tool," *Technology 2005*, NASA, Washington, DC, Oct. 1995.

[21] Picone, J. M., Hedin, A. E., Drob, D. P., and Aikin, A. C., "The NRLMSISE-00 Empirical Model of the Atmosphere: Statistical Comparisons and Scientific Issues," *Journal of Geophysical Research*, Vol. 107, No. A12, Dec. 2002, pp. 15.1–15.16.

[22] Reigber, C., Bock, R., Förste, C., Grunwaldt, L., Jakowski, N., Lühr, H., Schwintzer, P., and Tilgner, C., "CHAMP Phase B, Executive Summary," German Research Centre for Geosciences Tech. Rept. STR96/13, Potsdam, Germany, Nov. 1996.

[23] Kuang, D., Bar-Sever, Y., Bertiger, W., Desai, S., Haines, B., Iijima, B., Kruizinga, G., Meehan, T., and Romans, L., "Precise Orbit Determination for CHAMP Using GPS Data from BlackJack Receiver," *Proceedings of the Institute of Navigation 2001 National Technical Meeting*, Inst. of Navigation, Manassas, VA, Jan. 2001, pp. 762–770.

[24] Sutton, E. K., "Normalized Force Coefficients for Satellites with Elongated Shapes," *Journal of Spacecraft and Rockets*, Vol. 46, No. 1, Jan.–Feb. 2009, pp. 112–116.
doi:10.2514/1.40940

[25] "U.S. Standard Atmosphere, 1976," NASA Tech. Rept. TMX-74335, 1976.

C. McLaughlin
Associate Editor